Journal of Fluorescence (2021) 31:307–314
https://doi.org/10.1007/s10895-020-02656-2

SHORT COMMUNICATION

Spectroscopic Analysis of Fe Ion-Induced Fluorescence Quenching of the Green Fluorescent Protein ZsGreen

In Jung Kim [1,2] · Yongbin Xu [3,4] · Ki Hyun Nam [5]

Received: 6 August 2020 / Accepted: 23 November 2020 / Published online: 7 January 2021

Abstract

The fluorescence of fluorescent proteins (FPs) is quenched when they are exposed to certain transition metals, which makes them promising receptor materials for metal biosensors. In this study, we report the spectroscopic analysis of metal-induced fluorescence quenching of the fluorescent protein ZsGreen from *Zoanthus* sp. The fluorescence of ZsGreen was reduced to 2%, 1%, and 20% of its original intensity by Fe^{2+}, Fe^{3+}, and Cu^{2+}, respectively. Metal titration experiments indicated that the dissociation constants of Fe^{2+}, Fe^{3+}, and Cu^{2+} for ZsGreen were 11.5, 16.3, and 68.2 μM, respectively. The maximum binding capacities of ZsGreen for Fe^{2+}, Fe^{3+}, and Cu^{2+} were 103.3, 102.2, and 82.9, respectively. Reversibility experiments indicated that the fluorescence of ZsGreen, quenched by Fe^{2+} and Fe^{3+}, could be recovered, but only to about 15% of its original intensity, even at a 50-fold molar excess of EDTA. In contrast, the fluorescence quenched by Cu^{2+} could be recovered up to 89.47% of its original intensity at a Cu^{2+}: EDTA ratio of 1:5. The homology model of ZsGreen revealed that the protein does not share any metal-binding sites with previously reported FPs, suggesting that ZsGreen contains unprecedented binding sites for fluorescence quenching metal ions.

Keywords Metal biosensor · Fluorescent protein · ZsGreen · Fluorescence quenching · Reversibility · Homology modeling

Introduction

Fluorescent proteins (FPs) are useful optical markers for tracking target molecules and they are widely applied in cell and molecular biology [1–3]. FPs allow the localization of protein expression and visualization of the transport of target molecules [4, 5]. FPs are used in combination with other fluorescent partners to observe target molecule interactions, such as protein-protein or protein-nucleic acid interactions in living cells [6, 7]. FPs emit strong fluorescence even at low concentrations. Therefore, they are not only used as biosensor markers [8], but also as screening probes to monitor the expression of membrane proteins with low expression levels [9]. Beyond life sciences, fluorescent proteins have been used for breeding green pigs and cats, and genetically modified fluorescent fishes are already found in home aquariums [10]. In addition, FP-integrated white LED displays have been investigated for potential industrial applications [11]. The extended applications of FPs not only include the identification of the molecular mechanisms of FPs, but also the engineering of these proteins, with new fluorescent proteins being discovered constantly [2, 12–15].

Green fluorescent protein (GFP)-like proteins have a β-barrel architecture, and a tripeptide inside the β-barrel forming the unique chromophore through cyclization, dehydration, and oxidation during the folding process [1]. The chromophores of natural FPs are based on two rings linked through a double bond and derived from the tyrosine-glycine dipeptide [2]. In general, the optical properties of FPs are determined by the chromophore and the surrounding hydrogen bond network that interacts with it [1, 16]. In addition, the fluorescence of

✉ Ki Hyun Nam
structures@postech.ac.kr

1 Division of Biotechnology, College of Life Sciences and Biotechnology, Korea University, Seoul 02841, Republic of Korea

2 Present address: Department of Biotechnology and Enzyme Catalysis, Institute of Biochemistry, University of Greifswald, D-17487 Greifswald, Germany

3 Department of Bioengineering, College of Life Science, Dalian Minzu University, Dalian 116600, Liaoning, China

4 Key Laboratory of Biotechnology and Bioresources Utilization, Ministry of Education, Dalian Minzu University, Dalian, China

5 Department of Life Science, Pohang University of Science and Technology, Pohang 37673, Republic of Korea

FPs can be strongly influenced by external factors, such as pH and metals [17–23]. Therefore, FPs have potential applications as pH indicators and metal biosensors [17–25]. FPs undergo fluorescence quenching by specific transition metals, and therefore they are considered for metal biosensor probes [17, 22–24, 26, 27].

Spectroscopic analysis of various FPs, such as BFPms1, DsRed, Dronpa, iq-mEmerald, AmCyan, mOrange, and ZsYellow [17–19, 21–25], enabled understanding of the metal-induced fluorescence quenching mechanisms as well as their potential as metal biosensors. The fluorescence of most FPs exhibited the highest sensitivity to Cu^{2+}; however, their fluorescence could be restored using EDTA [17–19, 21–24]. Each FP differs in its sensitivity to metals, and each metal has varying mechanisms for quenching. For example, in BFPms1, Cu^{2+} binds directly to the chromophore and quenches its fluorescence [25]. In iq-mEmerald and Dronpa, fluorescence quenching occurs when the metal interacts with two histidine residues located on the β-barrel surface of the proteins [21, 22]. On the other hand, the fluorescence of ZsYellow is quenched by Cu^{2+} in a distance-dependent manner with low sensitivity [24]. Based on the crystal structure of ZsYellow soaked in Cu^{2+}, it was suggested that quenching could occur even without metal binding when the distance between Cu^{2+} and the chromophore is reduced due to high metal concentrations. The diverse mechanisms of metal-induced fluorescence quenching of FPs require continuous investigations of metal-induced fluorescence quenching of new FPs, for the development of FP-based metal biosensor probes.

In particular, ions of iron are involved in many physiologically important processes such as respiration, oxygen transport, signal transduction, and enzymatic reactions that rely on their ability to activate molecular oxygen [28]. Several chemical tools for the detection of these ions using fluorescent or chromogenic probe have been developed [28]; however, no FP has exhibited fluorescence quenching with sensitivity high enough for it to be utilized as a biosensor.

GFP FP506 from *Zoanthus* sp. has excitation and emission maxima at 492 and 506 nm, respectively [29]. ZsGreen is a GFP engineered from GFP FP506 in which the amino acid Asn65 is replaced by a Met, improving the fluorescence emission characteristics (excitation and emission maxima at 496 and 506 nm, respectively) [30]. ZsGreen is widely used as an optical probe in molecular and cell biology [31–33]; however, metal-induced fluorescence quenching of this protein has not been elucidated. In this study, we report the spectroscopic analysis of metal-induced fluorescence quenching of ZsGreen. Fe^{2+}-, Fe^{3+}- and Cu^{2+}-titration experiments were performed, followed by EDTA treatment to investigate the reversibility of metal-induced fluorescence quenching. To identify metal-binding sites in ZsGreen, homology modeling was performed to compare the structure of ZsGreen with those of previously reported metal-bound FPs. Our results provide a better understanding of the optical properties of ZsGreen in the presence of metal ions and insights into the development of FP-based metal biosensors.

Materials and Methods

Protein Preparation

The expression vector encoding ZsGreen (Clontech) was transformed into *Escherichia coli* BL21(DE3). The cells were grown on LB agar plates supplemented with 50 μg/mL ampicillin. A single colony was transferred into 5 mL LB medium with 50 μg/mL ampicillin and incubated with shaking overnight at 37 °C. The overnight culture was inoculated into 1 L LB medium supplemented with 50 μg/mL ampicillin and incubated with vigorous shaking at 200 rpm at 37 °C. When the culture reached an optical density of 0.6–0.8 at 600 nm, protein expression was induced using 0.5 mM isopropyl β-d-1-thiogalactopyranoside (IPTG), and the culture was incubated overnight at 18 °C. The cells were then harvested by centrifugation at 4000 rpm for 20 min and subsequently suspended in 50 mM Tris-HCl (pH 8.0) and 200 mM NaCl. After sonication, the supernatant was heat-treated at 50 °C for 30 min to denature soluble proteins from the *Escherichia coli* host [23, 34], and then centrifuged at 14,000 rpm for 30 min. Heat-treatment was performed twice. Supernatants were concentrated using an Amicon concentration device (Millipore, cutoff: 10 kDa) and loaded on a Sephacryl 100-HR column (GE Healthcare) equilibrated with 10 mM Tris-HCl (pH 8.0) and 200 mM NaCl. Protein concentration was measured using the Bradford assay using a Synergy H1 microplate reader (BioTek), at 25 °C.

Spectroscopic Analysis

The maximum fluorescence excitation and emission wavelengths for purified ZsGreen were obtained using the spectrum scan method. For the fluorescence emission measurements, purified ZsGreen was excited at 470 nm, and the fluorescence emission was measured at 520 nm. Fluorescence emission of all samples, in 96-well plates, was measured using a Synergy H1 microplate reader (BioTek) after orbital shaking for 10 s. All experiments were performed in triplicate at 25 °C.

Screening Metal-Induced Quenching

To investigate the effect of different metal ions on fluorescence, 10 μM of purified ZsGreen in 10 mM Tris-HCl (pH 8.0) and 200 mM NaCl was mixed with 1 mM metal solution (LiCl, NaCl, $MgCl_2$, $CaCl_2$, $MnCl_2$, $FeCl_2$, $FeCl_3$, $CoCl_2$, $NiCl_2$, $CuCl_2$, $ZnCl_2$, $CdCl_2$, and $CeCl_2$) at a ratio of

1:1. Each mixture was incubated for five minutes at room temperature and placed on a LED transilluminator (Maestrogen) to visually monitor the fluorescence intensity using an excitation of 470 nm. For fluorescence measurement, 0.87 μM of purified ZsGreen in 10 mM Tris-HCl (pH 8.0) and 200 mM NaCl was mixed with 1 mM metal solution (LiCl, NaCl, $MgCl_2$, $CaCl_2$, $MnCl_2$, $FeCl_2$, $FeCl_3$, $CoCl_2$, $NiCl_2$, $CuCl_2$, $ZnCl_2$, $CdCl_2$, and $CeCl_2$) at a ratio of 1:1. The fluorescence emission spectra were recorded for each solution.

Titration Experiment

For titration experiments, 50 μL ZsGreen solution (0.87 μM) was mixed with an equal volume of 0, 0.01, 0.1, 1.0, 10, 100, 1000, and 10,000 μM $FeCl_2$, $FeCl_3$, or $CuCl_2$. After the mixture was incubated for five minutes at room temperature, fluorescence was measured. The relative fluorescence quenching (%) is defined as follows:

$$(1-F/F_0) \times 100,$$

where F and F_0 are the fluorescence intensities of ZsGreen in the presence and absence of the quenching metal ions, respectively. Titration data were analyzed using SigmaPlot 12.3 software (Systat Software, Erkrath, Germany). Data were fitted according to the Langmuir equation as follows using nonlinear least square regression analysis:

$$\text{Relative fluorescence quenching } (\%) = \frac{B_{max}\,[M]_{unbound}}{K_d + [M]_{unbound}}$$

where B_{max} represents the maximum binding capacity of ZsGreen for metal ions, K_d is the dissociation constant between ZsGreen and metal ions (μM), and $[M]_{unbound}$ is the concentration of unbound metal ions (μM). If the total metal ion concentration is in large molar excess compared to that of ZsGreen, it can be assumed that $[M]_{unbound}$ is approximately equal to $[M]_{total}$. Therefore, a large excess of metal ions was used to obtain the values for K_d and B_{max} from the Langmuir isotherm.

Reversibility of Metal-Induced Fluorescence Quenching

To investigate the reversibility of the metal-induced fluorescence quenching, we prepared the ZsGreen in a quenched state of fluorescence by mixing 50 μL ZsGreen (0.87 μM) with 50 μL metal solution (1 mM Fe^{2+}, 1 mM Fe^{3+}, or 10 mM Cu^{2+}) followed by incubation for five minutes at room temperature. The quenching in each mixture was verified through measuring the fluorescence emission. Then, 50 μL EDTA (0.1, 0.5, 1.0, 5.0, 10, and 50 mM) was added to the quenched solution. After incubation for five minutes at 25 °C, fluorescence emission was measured.

Homology Modeling

The homology model of ZsGreen was generated using the SWISS-MODEL server [35]. The crystal structure of GFP-like fluorescent chromoprotein FP506 (PDB code: 2OJK) [36] was used as a template. The geometry of the ZsGreen model was validated using MolProbity [37]. The model structure was visualized using PyMOL (http://pymol.org/). Amino acid sequence alignments were performed using ClustalW [38] and visualized using ESPript [39].

Results and Discussion

Fe^{2+}- and Fe^{3+}-Induced Fluorescence Quenching

First, the optimum fluorescence excitation and emission wavelengths of purified ZsGreen were scanned. Maximum excitation and emission peaks were observed at 491 and 505 nm, respectively (Fig. 1a). Compared with the previously published maximum excitation and emission wavelengths of ZsGreen (λ_{ex} = 496 nm and λ_{em} = 506 nm), the present wavelengths were blue-shifted by 5 and 1 nm, respectively.

When the fluorescence of an FP is quenched by a metal, the protein exhibits metal type-specific spectral properties (quenching intensities.) [22, 23]. To investigate the fluorescence quenching of ZsGreen by metal ions, purified protein solution was mixed with various metal ions (Li^+, Na^+, Mg^{2+}, Ca^{2+}, Mn^{2+}, Fe^{2+}, Fe^{3+}, Co^{2+}, Ni^{2+}, Cu^{2+}, Zn^{2+}, Cd^{2+}, and Ce^{2+}). Fluorescence quenching was first visually monitored by exposing the solutions to LED light at 470 nm. In the presence of Fe^{2+} and Fe^{3+}, the ZsGreen solution did not fluoresce at all and Cu^{2+} markedly reduced the fluorescence intensity compared to that of the metal-free protein solution (Fig. 1b). These mixtures were further quantitatively analyzed through fluorescence emission measurements (Fig. 1c). The fluorescence intensity of ZsGreen was decreased to 1.1% and 3.5% of its maximum intensity (metal-free ZsGreen) by Fe^{2+} and Fe^{3+}, respectively. Cu^{2+} reduced the fluorescence intensity to 22.8%. Co^{2+}, Ni^{2+}, Zn^{2+}, and Cd^{2+} quenched the fluorescence intensity by 22.6%, 12.6%, 37.3%, and 19.0%, respectively. Li^+, Na^+, Mg^{2+}, Ca^{2+}, and Mn^{2+} exhibited modest quenching and reduced the fluorescence intensity only by 5.6%, 2.9%, 4.4%, 4.6%, and 8.0%, respectively. On the other hand, Ce^{2+} increased the fluorescence intensity by 1.4%. Therefore, we concluded that the fluorescence of ZsGreen was highly sensitive to quenching by Fe^{2+}, Fe^{3+}, and Cu^{2+}.

Titration Experiment

To better understand the mechanism of quenching, we performed Fe^{2+}-, Fe^{3+}- and Cu^{2+}-titration experiments with ZsGreen (Fig. 2). Fe^{2+}-titration showed that at a concentration

of 0.1, 1.0, and 10 mM Fe^{2+}, the ZsGreen fluorescence was quenched by 92.6%, 98.9%, and 99.8%, respectively (Fig. 2a). At a concentration of 10 μM Fe^{2+}, the fluorescence intensity was reduced to 25.4% of its original value, whereas at concentrations lower than 1 μM, the intensity was reduced by less than 6.5%. During Fe^{3+}-titration, Fe^{3+} concentrations of 0.1, 1.0, and 10 mM, quenched the ZsGreen fluorescence by 83.2%, 98.1%, and 99.6%, respectively (Fig. 2b). At a concentration of 10 μM Fe^{3+}, the fluorescence intensity was reduced to 17.8% of its maximum intensity, whereas at lower Fe^{2+} concentrations (≤ 1 μM) it was only reduced by less than 10%. During the titration with Cu^{2+}, metal concentrations of 1.0 and 10 mM decreased the ZsGreen fluorescence by 78.2% (Fig. 2c). At a concentration of 100 μM Cu^{2+}, the fluorescence intensity was reduced to 31.4%, and at concentrations lower than 10 μM, the intensity was reduced by less than 12%.

Based on the titration experiments, the dissociation constant (K_d) and maximum binding capacity (B_{max}) were obtained from the Langmuir equation. Only metal ions with a large molar excess concentration relative to that of ZsGreen were used for obtaining the K_d and B_{max} values to satisfy the assumption that $[M]_{unbound}$ is approximately equal to $[M]_{total}$, as described in the Methods section. Theoretically, the affinity of a protein for a ligand is inversely proportional to the value of K_d. The K_d values of Fe^{2+}, Fe^{3+}, and Cu^{2+} for ZsGreen were 11.5, 16.3, and 68.2 μM, respectively. B_{max} values of ZsGreen in the presence of Fe^{2+}, Fe^{3+}, and Cu^{2+} were 103.3, 102.2, and 82.9, respectively. Taken together, Fe^{2+} and Fe^{3+} exhibited a similar behavior in terms of both binding affinity and the maximum binding capacity for ZsGreen, which were approximately 5- and 1.2-fold higher than that of Cu^{2+}, respectively.

Reversibility of Metal-Induced Quenching

The fluorescence quenched by metals can be recovered using chelating agents such as EDTA [22, 23]. This reversibility of metal-induced fluorescence quenching renders FPs attractive as sustainable materials for metal biosensors. To investigate the reversibility of fluorescence quenching, we prepared ZsGreen solutions with quenched fluorescence by adding the 1 mM Fe^{2+}, 1 mM Fe^{3+}, or 10 mM Cu^{2+}. Subsequently, varying concentrations of EDTA (0.1–50 mM) were added to recover the fluorescence of ZsGreen (Fig. 3). Fe^{2+} quenched the fluorescence of ZsGreen to 2.0% of its original level (metal-free ZsGreen); however, the addition of 10 and 50 mM EDTA recovered the fluorescence to about 8.1% and 15.9%, respectively, of its original intensity (Fig. 3a). When 1 and 5 mM EDTA was added, fluorescence was recovered to only 6.1% and 6.0%, respectively, of its maximum intensity, whereas no detectable recovery occurred at lower EDTA concentrations (<1 mM). Similarly, Fe^{3+} reduced the fluorescence of ZsGreen by up to 98.9% (Fig. 3b). Addition of 5, 10, and 50 mM EDTA recovered the fluorescence to about 5.2%, 6.6%, and 13.3%, respectively, of its original intensity (Fig. 3b). At low EDTA concentration (≤ 1 mM), no fluorescence recovery was observed. Cu^{2+} quenched the ZsGreen

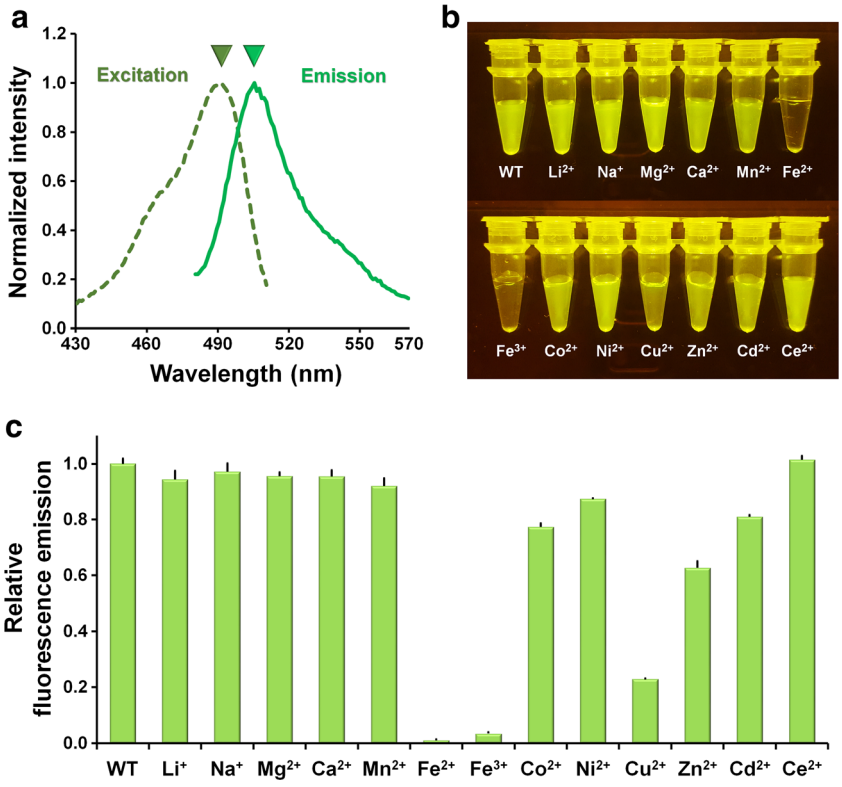

Fig. 1 Spectral analysis of fluorescence quenching of ZsGreen by metal ions. a Normalized fluorescence spectral scan of purified ZsGreen. Fluorescence excitation (dotted line) and emission (solid line) spectra of purified ZsGreen (arrowheads indicate the maxima at 491 and 505 nm). **b** Visual observation of metal-induced fluorescence quenching using LED light. **c** Measurement of the fluorescence emission of ZsGreen in the presence of various metals

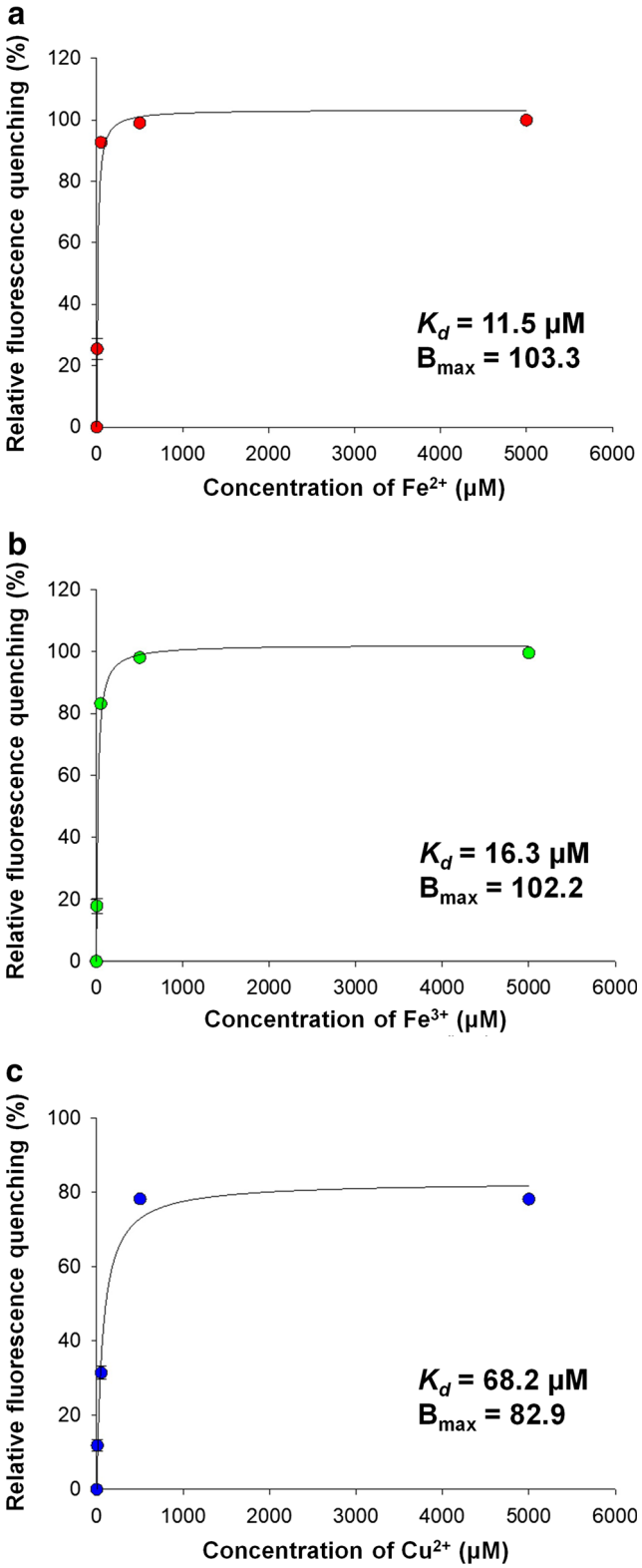

◀ **Fig. 2 Metal titration of ZsGreen.** Titration of ZsGreen with **a** Fe^{2+}, **b** Fe^{3+}, and **c** Cu^{2+}. Fluorescence of ZsGreen was measured in the presence of 0, 0.01, 0.1, 1, 10, 100, 1000, and 10,000 μM metal ions. Relative fluorescence quenching (%) was calculated as follows: $(1 - F / F_0) \times 100$, where F and F_0 are the fluorescence intensities of ZsGreen in the presence and absence of the quenching metal ions, respectively. Data fitting was performed using non-linear least square regression analysis based on Langmuir isotherm

fluorescence by 82.0% (Fig. 3b); however, the addition of 5, 10, and 50 mM EDTA, recovered the fluorescence to about 26.1%, 32.3%, and 89.5%, respectively, of its maximum intensity. On the other hand, EDTA concentrations lower than 1 mM did not recover ZsGreen fluorescence. In summary, the fluorescence of ZsGreen quenched by Fe^{2+} and Fe^{3+} could only be recovered to about 15% of its original intensity even

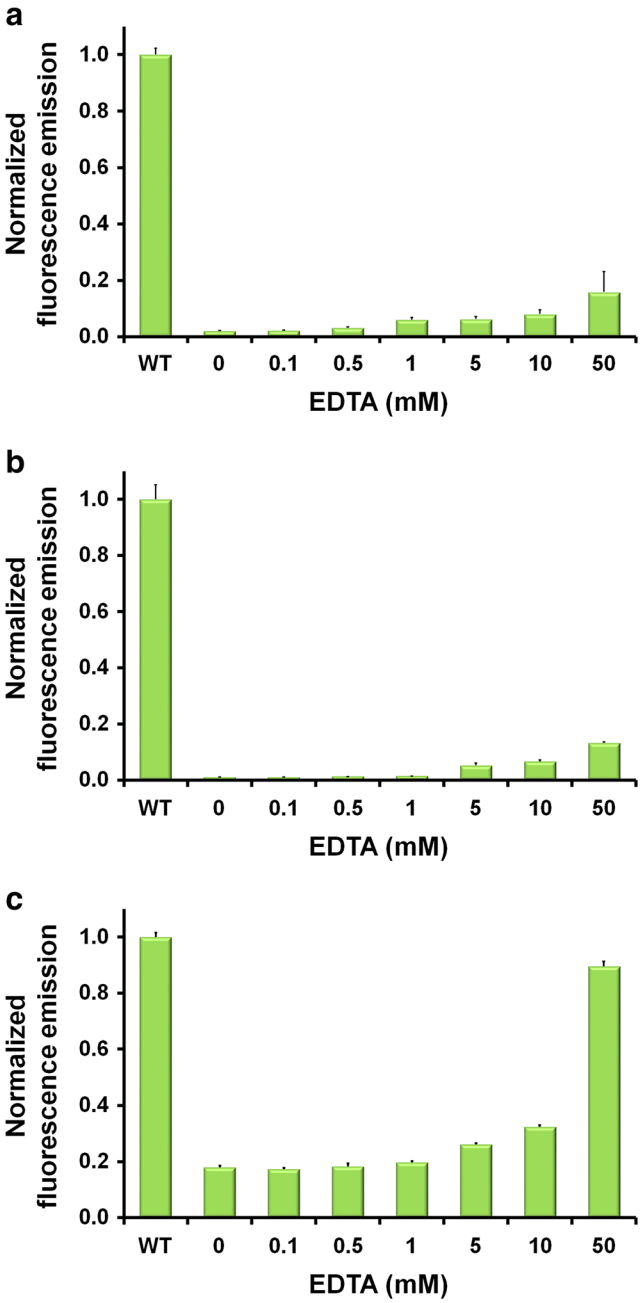

Fig. 3 Reversibility of metal-induced fluorescence quenching. **a** Fe^{2+}-, **b** Fe^{3+}-, and **c** Cu^{2+}-induced quenching of ZsGreen was recovered by the addition of EDTA

with a 50-fold molar excess of EDTA. On the other hand, Cu^{2+}-quenched fluorescence was recovered to about 90% of its maximum intensity with a 5-fold molar excess of EDTA.

Analysis of the Homology Model of ZsGreen

Currently, three different mechanisms have been suggested for metal-induced FP fluorescence quenching based on crystal structures [21, 22, 24, 25]: (1) The quenching metal binds directly to the chromophore of FP. (2) The quenching metal binds to the β-barrel surface of the FP. (3) At high metal concentrations, the quenching metals come very close to the FP and quench its fluorescence without direct interaction. To better understand the mechanism of metal binding with ZsGreen, we generated a homology model and compared it with previously reported crystal structures of BFPms1 [25], Dronpa [22], iq-mEmerald [21], and ZsYellow [24]. In BFPms1, the quenching Cu^{2+} is directly bound to the chromophore through an engineered solvent channel between the β7- and β8-strands [25] (Fig. 4a). In the homology model of ZsGreen, such a channel at the surface of the protein, through which metals could directly access the chromophore, is lacking (Fig. 4a). Therefore, it is suggested that quenching metal ions do not directly interact with the chromophore of ZsGreen. In Dronpa and iq-mEmerald, histidine residues on the β-barrel surface interact with the fluorescence quenching metals; these histidines are about 14.4–16.4 Å distant from the center of the chromophore [21, 22]. Superimposition of the ZsGreen homology model and the structure of Dronpa revealed that the amino acid positions His194, His210, and His212 in Dronpa, which are involved in the binding of quenching metals, were occupied by Lys203, Thr220, and His222, respectively, in the ZsGreen structure. Although His222 of ZsGreen was located at a position equivalent to that of the metal-binding residue His212 in Dronpa, a second histidine residue around His222 was missing for metal binding (Fig. 4b). Similarly, the superimposition of the ZsGreen model and the structure of iq-mEmerald indicated that the metal-binding positions His202 and His204 in iq-mEmerald were occupied by Gln201 and Lys203, respectively, in ZsGreen, indicating that ZsGreen does not contain a metal-binding site similar to that in iq-mEmerald (Fig. 4c). In the crystal structure of ZsYellow quenched by Cu^{2+}, no Cu^{2+} ion was observed, suggesting that fluorescence quenching occurred due to the proximity between Cu^{2+} ions and the chromophore, without direct interaction [24]. Owing to the observed high binding affinities of Fe^{2+} and Fe^{3+} with ZsGreen, we assumed that the protein had binding sites for these ions. However, Cu^{2+} had a low binding affinity for ZsGreen; therefore, it was considered that Cu^{2+} ions exhibit a quenching mechanism similar to that observed in ZsYellow. Taken together, the results suggested that ZsGreen lacked the metal-binding sites of previously reported FPs and the possible presence of a novel metal-binding site for Fe^{2+} and Fe^{3+}.

Conclusion

We reported the spectroscopic analysis of metal-induced fluorescence quenching of ZsGreen. Previous studies indicated that the fluorescence of FPs is highly sensitive to quenching by Cu^{2+} ions. In the case of ZsGreen, Cu^{2+} reduced the fluorescence intensity, but Fe^{2+} and Fe^{3+} induced considerably higher fluorescence quenching compared with that of Cu^{2+}

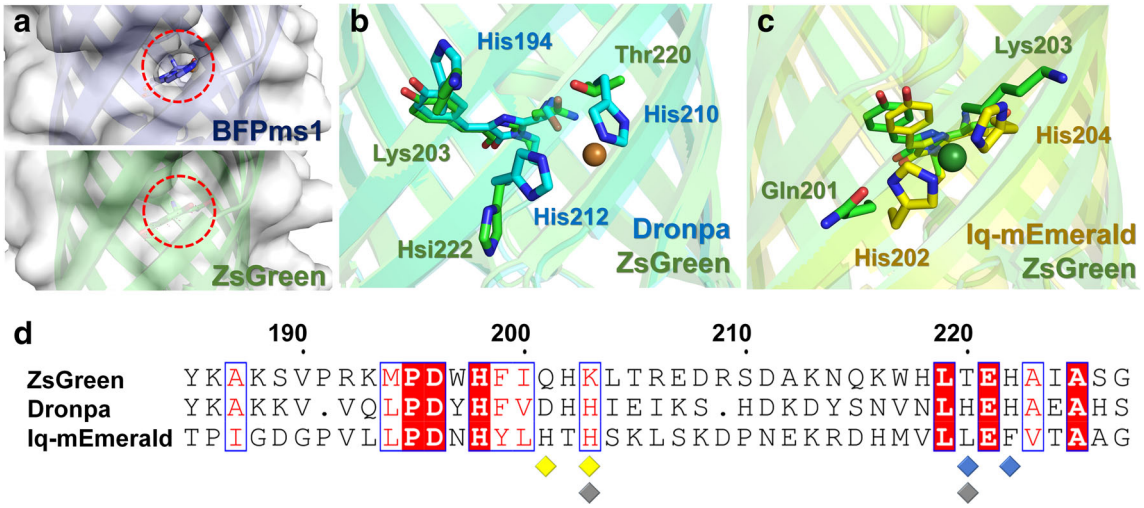

Fig. 4 Structural comparisons of the ZsGreen homology model with the structures of BFPms1, Dronpa, and iq-mEmerald. a Comparison of the β-barrel surface between BPFms1 (PDB code: 1KYS) and ZsGreen. Superimposition of the ZsGreen homology model and the structures of (**b**) Dronpa (PDB code: 5HZT), and (**c**) iq-mEmerald (PDB code: 4KW4). **d** Partial sequence alignments of ZsGreen, Dronpa, and iq-mEmerald. The metal-binding sites of Dronpa (blue, Cu^{2+}; gray, Co^{2+}/Ni^{2+}) and iq-mEmerald (yellow, Ni^{2+}) are indicated by diamonds

and other metals. These results indicated that ZsGreen could potentially be applied as a biosensor probe for detection of iron. However, despite the different oxidation states of Fe^{2+} and Fe^{3+}, their quenching effects on ZsGreen fluorescence did not differ in the present spectroscopic experiments. The fluorescence of ZsGreen quenched by both Fe^{2+} and Fe^{3+} could not be effectively restored, whereas the fluorescence quenched by Cu^{2+} was recovered up to 89.5% of its original intensity, using EDTA. Meanwhile, the partial recovery of Fe^{2+}/Fe^{3+}-quenched fluorescence using EDTA indicated that the metal ions are located on the surface of ZsGreen. To improve the efficiency of recovery for biosensor applications, higher concentrations of EDTA, longer incubation times, or the use of another Fe chelating method should be explored.

Structural analysis of the homology model of ZsGreen suggested that ZsGreen possesses novel binding sites for Fe^{2+}/Fe^{3+} that are distinct from the metal-binding sites found in Dronpa and iq-mEmerald. Due to the low binding affinity of Cu^{2+} for ZsGreen, fluorescence quenching by Cu^{2+} is considered to be caused through high metal concentrations without specific binding, as observed in the case of ZsYellow fluorescence quenching by Cu^{2+} [24]. Cu^{2+} favors histidine-containing binding sites on the FP surface, whereas Fe^{2+} and Fe^{3+} may not bind to histidine residues, because of coordination geometry considerations. To identify the metal-binding sites of ZsGreen, the crystal structure of ZsGreen complexed with Fe^{2+}, Fe^{3+}, and Cu^{2+} is required. Nevertheless, our results provide important insights for the future development of metal biosensors, especially that of Fe^{2+}/Fe^{3+} biosensors.

Authors' Contributions Conceptualization, K.H.N.; Biochemical studies, I.J.K.; structure analysis, Y.X. and K.H.N.; manuscript writing, I.J.K. and K.H.N. All authors read and approved the final manuscript.

Funding This work was supported by the National Research Foundation of Korea (NRF) grant funded by the Korea government (MEST) (NRF-2017R1D1A1B03033087 and NRF-2017M3A9F6029736).

Data Availability The datasets generated or analyzed during the current study are available from the corresponding author on reasonable request.

Compliance with Ethical Standards

Conflict of Interest The authors declare that they have no conflict of interest.

References

1. Tsien RY (1998) The green fluorescent protein. Annu Rev Biochem 67:509–544
2. Remington SJ (2011) Green fluorescent protein: a perspective. Protein Sci 20:1509–1519
3. Zimmer M (2002) Green fluorescent protein (GFP): applications, structure, and related photophysical behavior. Chem Rev 102:759–781
4. Collings DA (2013) Subcellular localization of transiently expressed fluorescent fusion proteins. Methods Mol Biol 1069: 227–258
5. Chalfie M (1995) Green fluorescent protein. Photochem Photobiol 62:651–656
6. Bajar BT, Wang ES, Zhang S, Lin MZ, Chu J (2016) A guide to fluorescent protein FRET pairs. Sensors (Basel) 16:1488
7. Lu K, Vu CQ, Matsuda T, Nagai T (2019) Fluorescent protein-based indicators for functional super-resolution imaging of biomolecular activities in living cells. Int J Mol Sci 20:5784
8. Stepanenko OV, Verkhusha VV, Kuznetsova IM, Uversky VN, Turoverov KK (2008) Fluorescent proteins as biomarkers and biosensors: throwing color lights on molecular and cellular processes. Curr Protein Pept Sci 9:338–369
9. Backmark AE, Olivier N, Snijder A, Gordon E, Dekker N, Ferguson AD (2013) Fluorescent probe for high-throughput screening of membrane protein expression. Protein Sci 22:1124–1132
10. Chudakov DM, Matz MV, Lukyanov S, Lukyanov KA (2010) Fluorescent proteins and their applications in imaging living cells and tissues. Physiol Rev 90:1103–1163
11. Press DA, Melikov R, Conkar D, Firat-Karalar EN, Nizamoglu S (2016) Fluorescent protein integrated white LEDs for displays. Nanotechnology 27:45LT01
12. Xu Y, Hwang KY, Nam KH (2018) Spectral and structural analysis of large stokes shift fluorescent protein dKeima570. J Microbiol 56: 822–827
13. Seward HE, Bagshaw CR (2009) The photochemistry of fluorescent proteins: implications for their biological applications. Chem Soc Rev 38:2842–2851
14. Kim SE, Hwang KY, Nam KH (2019) Spectral and structural analysis of a red fluorescent protein from Acropora digitifera. Protein Sci 28:375–381
15. Saeed S, Mehreen H, Gerlevik U, Tariq A, Manzoor S, Noreen Z, Sezerman U, Bokhari H (2020) HriGFP novel Flourescent protein: expression and applications. Mol Biotechnol 62:280–288
16. Pal PP, Bae JH, Azim MK, Hess P, Friedrich R, Huber R, Moroder L, Budisa N (2005) Structural and spectral response of Aequorea victoria green fluorescent proteins to chromophore fluorination. Biochemistry 44:3663–3672
17. Eli P, Chakrabartty A (2006) Variants of DsRed fluorescent protein: development of a copper sensor. Protein Sci 15:2442–2447
18. Sumner JP, Westerberg NM, Stoddard AK, Hurst TK, Cramer M, Thompson RB, Fierke CA, Kopelman R (2006) DsRed as a highly sensitive, selective, and reversible fluorescence-based biosensor for both Cu^{+} and Cu^{2+} ions. Biosens Bioelectron 21:1302–1308
19. Peterffy JP, Szabo M, Szilagyi L, Lanyi S, Abraham B (2015) Fluorescence of a Histidine-modified enhanced green fluorescent protein (EGFP) effectively quenched by Copper(II) ions. Part II Molecular Determinants. J Fluoresc 25:871–883
20. Bae JE, Kim IJ, Nam KH (2017) Disruption of the hydrogen bonding network determines the pH-induced non-fluorescent state of the fluorescent protein ZsYellow by protonation of Glu221. Biochem Biophys Res Commun 493:562–567
21. Yu X, Strub MP, Barnard TJ, Noinaj N, Piszczek G, Buchanan SK, Taraska JW (2014) An engineered palette of metal ion quenchable fluorescent proteins. PLoS One 9:e95808
22. Kim IJ, Kim S, Park J, Eom I, Kim S, Kim JH, Ha SC, Kim YG, Hwang KY, Nam KH (2016) Crystal structures of Dronpa complexed with quenchable metal ions provide insight into metal biosensor development. FEBS Lett 590:2982–2990
23. Bae JE, Kim IJ, Nam KH (2018) Spectroscopic Analysis of the Cu^{2+}-Induced Fluorescence Quenching of Fluorescent Proteins AmCyan and mOrange2. Mol Biotechnol 60:485–491
24. Kim IJ, Xu Y, Nam KH (2020) Spectroscopic and structural analysis of Cu^{2+}-induced fluorescence quenching of ZsYellow. Biosensors (Basel) 10:29

25. Barondeau DP, Kassmann CJ, Tainer JA, Getzoff ED (2002) Structural chemistry of a green fluorescent protein Zn biosensor. J Am Chem Soc 124:3522–3524
26. Lee W, Kim H, Kang Y, Lee Y, Yoon Y (2019) A biosensor platform for metal detection based on enhanced green fluorescent protein. Sensors (Basel) 19:1846
27. Martinez AR, Heil JR, Charles TC (2019) An engineered GFP fluorescent bacterial biosensor for detecting and quantifying silver and copper ions. Biometals 32:265–272
28. Hirayama T, Nagasawa H (2017) Chemical tools for detecting Fe ions. J Clin Biochem Nutr 60:39–48
29. Matz MV, Fradkov AF, Labas YA, Savitsky AP, Zaraisky AG, Markelov ML, Lukyanov SA (1999) Fluorescent proteins from nonbioluminescent Anthozoa species. Nat Biotechnol 17:969–973
30. Wenck A, Pugieux C, Turner M, Dunn M, Stacy C, Tiozzo A, Dunder E, van Grinsven E, Khan R, Sigareva M, Wang WC, Reed J, Drayton P, Oliver D, Trafford H, Legris G, Rushton H, Tayab S, Launis K, Chang YF, Chen DF, Melchers L (2003) Reef-coral proteins as visual, non-destructive reporters for plant transformation. Plant Cell Rep 22:244–251
31. Bryda EC, Men H, Davis DJ, Bock AS, Shaw ML, Chesney KL, Hankins MA (2019) A novel conditional ZsGreen-expressing transgenic reporter rat strain for validating Cre recombinase expression. Sci Rep 9:13330
32. McCann JV, Liu A, Musante L, Erdbrugger U, Lannigan J, Dudley AC (2019) A miRNA signature in endothelial cell-derived extracellular vesicles in tumor-bearing mice. Sci Rep 9:16743
33. Gwon YD, Strand M, Lindqvist R, Nilsson E, Saleeb M, Elofsson M, Overby AK, Evander M (2020) Antiviral activity of Benzavir-2 against emerging Flaviviruses. Viruses 12:351
34. Nam KH, Kwon OY, Sugiyama K, Lee WH, Kim YK, Song HK, Kim EE, Park SY, Jeon H, Hwang KY (2007) Structural characterization of the photoswitchable fluorescent protein Dronpa-C62S. Biochem Biophys Res Commun 354:962–967
35. Biasini M, Bienert S, Waterhouse A, Arnold K, Studer G, Schmidt T, Kiefer F, Gallo Cassarino T, Bertoni M, Bordoli L, Schwede T (2014) SWISS-MODEL: modelling protein tertiary and quaternary structure using evolutionary information. Nucleic Acids Res 42: W252–W258
36. Pletneva N, Pletnev V, Tikhonova T, Pakhomov AA, Popov V, Martynov VI, Wlodawer A, Dauter Z, Pletnev S (2007) Refined crystal structures of red and green fluorescent proteins from the button polyp Zoanthus. Acta Crystallogr D Biol Crystallogr 63: 1082–1093
37. Williams CJ, Headd JJ, Moriarty NW, Prisant MG, Videau LL, Deis LN, Verma V, Keedy DA, Hintze BJ, Chen VB, Jain S, Lewis SM, Arendall WB 3rd, Snoeyink J, Adams PD, Lovell SC, Richardson JS, Richardson DC (2018) MolProbity: more and better reference data for improved all-atom structure validation. Protein Sci 27:293–315
38. Larkin MA, Blackshields G, Brown NP, Chenna R, McGettigan PA, McWilliam H, Valentin F, Wallace IM, Wilm A, Lopez R, Thompson JD, Gibson TJ, Higgins DG (2007) Clustal W and Clustal X version 2.0. Bioinformatics 23:2947–2948
39. Gouet P, Courcelle E, Stuart DI, Metoz F (1999) ESPript: analysis of multiple sequence alignments in PostScript. Bioinformatics 15: 305–308